Early Bone Healing around Different Implant Bulk Designs and Surgical Techniques: A Study in Dogs

Paulo G. Coelho, DDS, PhD;* Marcelo Suzuki, DDS;† Marcia V.M. Guimaraes, DDS, MS, DSc;‡ Charles Marin, DDS, MS;§ Rodrigo Granato, DDS, MS;§ Jose N. Gil, DDS, MS, DSc;§ Robert J. Miller, DMD¶

ABSTRACT

Purpose: To evaluate the bone healing response to different implant root shape designs in a dog model.

Materials and Methods: Three by eight millimeter screw-type short-pitch (SP) and large-pitch (LP) implants (Intra-Lock International, Boca Raton, FL, USA), and 4.5 × 6 mm plateau (P) implants (Bicon LLC, Boston, MA, USA) were placed along the proximal tibia of six dogs for 2 and 4 weeks. The combination of implant design and final osteotomy drilling resulted in healing chambers for the LP and P implants. The implants were nondecalcified processed to plates of ~30-μm thickness and were evaluated by optical microscopy for healing patterns and bone-to-implant contact (BIC). One-way analysis of variance at 95% level of significance and Tukey's test were utilized for multiple comparisons among the groups' BIC.

Results: Microscopy showed a ~150-μm region of newly deposited bone along the whole perimeter of SP implants, near the edge of the LP implant threads, and plateau tips for P implants. Rapid woven bone formation and filling was observed in regions where surgery and implant design resulted in healing chambers. No significant differences in BIC were observed ($p > .75$).

Conclusions: Different implant design/surgical protocol resulted in varied bone healing patterns. However, the BIC and bone morphology evolution between implant designs were comparable. Regardless of the combination between implant design and final osteotomy drilling, bone morphology evolution from 2 to 4 weeks was comparable.

KEY WORDS: dental implant, design, dog, in vivo, plateau root shape, screw root shape

INTRODUCTION

Osseointegration is a phenomenon where intimate contact between bone and biomaterials occurs at the optical microscopy level, enabling dental implants to replace load-bearing tooth organs and restore their form and intraoral function.[1] Specific to dental implantology, where implant therapy success ratios often exceed 90%,[2,3] basic and clinical research has attempted to decrease treatment time frames by reducing the healing period for the establishment of osseointegration.[4]

Over the last 40 years, surgical and prosthetic protocols substantially deviating from the classical two-stage protocol[5] have been suggested, typically under the rationale of implant design modifications that would enable improved healing and/or biomechanical behavior.[4,6–9] While a substantial amount of research has been devoted to increasing the implant surface biocompatibility and osseoconductivity,[4,6–10] little information has been published to date concerning the host-to-implant response considering the interplay between surgical protocols and implant bulk design.[11]

The vast majority of the dental implant systems commercially available presents a root shape where

*Department of Biomaterials and Biomimetics, New York University, New York, NY, USA; †Department of Prosthodontics and Operative Dentistry, Tufts School of Dental Medicine, Boston, MA, USA; ‡private practice, Guaratingueta, Sao Paulo, Brazil; §Department of Oral and Maxillofacial Surgery, Universidade Federal de Santa Catarina, Florianopolis, Brazil; ¶Department of Oral Implantology Atlantic Coast Dental Research Clinic, Palm Beach, FL, USA

Reprint requests: Dr. Paulo G. Coelho, Department of Biomaterials and Biomimetics, New York University, 345 24th Street, Room 804a, New York, NY 10010, USA; e-mail: pgcoelho@nyu.edu

DOI 10.1111/j.1708-8208.2009.00153.x

different types of thread design are employed for implant insertion and biomechanical fixation. Implant macroarchitecture has evolved to maximize initial stability in the osteotomy and to provide early stress distribution during the early healing phase. Primary stability of the implant allows early osteoblast proliferation without an intervening fibrous union. Typically, the surgical osteotomy for the placement of screw root shape implants comprises a series of drills of increasing diameter to final dimensions that may be either comparable or narrower in diameter to the implant internal thread diameter. Such intimate surgical fit between bone and screw root form implant results in the formation of a blood clot at the region between bone and implant surface, which is subsequently substituted by a new bone.[12] Then, the long-term stability of screw root shape implants is assured by bone modeling and remodeling processes,[12] a phenomenon that has rendered dental implantology one of the most successful treatment options in dentistry.

While screw root shape implants and surgical protocols that result in the placement of the implant surface in contact with the drilled bone (intimate fit) have been vastly used and researched, implant bulk designs combined with different surgical protocol and insertion methods have also been investigated. For example, screw root form implants, where the final surgical drilling diameter is slightly smaller than the thread outer diameter and larger than the thread inner diameter (resulting in a healing chamber) along with plateau root form implants (where healing chambers also result because of implant design and surgical drilling combination), have been investigated.[7,11] Following placement, the healing chambers are filled with a blood clot, which will result in new bone formation and biomechanical fixation. When large healing chambers are filled with a blood clot, a significantly different healing pattern will take place as compared with screw root shape implants.[7,11]

Irrespective of implant bulk design and its surgical drilling and insertion counterparts, lamellar bone morphology along regions in proximity with the implant surface will develop after several months in function, providing adequate biomechanical support for loading.[12–14] However, while the healing patterns have been described for both screw[1,12] and plateau root shapes,[7,11] temporal comparisons concerning bone histomorphology and histomorphometry are lacking in the literature.

This study was designed to evaluate the bone response and bone-to-implant contact (BIC) to different implant macrodesigns and their associated surgical drilling techniques at early implantation times in a dog tibia model.

MATERIALS AND METHODS

The different implant designs utilized were short-pitch (SP, $n = 12$, thread external diameter = 3.0 mm, thread internal diameter = 2.5 mm, dual acid-etched surface) and large-pitch (LP, $n = 12$, thread external diameter = 3.0 mm, thread internal diameter = 2.0 mm, dual acid-etched surface) MILO™ implants (Intra-Lock International, Boca Raton, FL, USA) of 3-mm diameter and 8-mm length, and plateau (P, $n = 12$, along the implant body, a minimum difference of 0.5 mm between outer and inner diameters, alumina-blasted/acid-etched surface) Integra-Ti™ implants of 4.5-mm diameter and 6-mm length (Bicon LLC, Boston, MA, USA) (Figure 1).

Following approval of the bioethics committee for animal experimentation at the Universidade Estadual de Sao Paulo in Sao Jose dos Campos, six male Doberman dogs of ~3.5 years of age weighing between 25 and 30 kg were acquired for the study.

The surgical region was the proximal tibia, with three implants placed in each limb. The first implant was inserted 2 cm below the joint line at the central

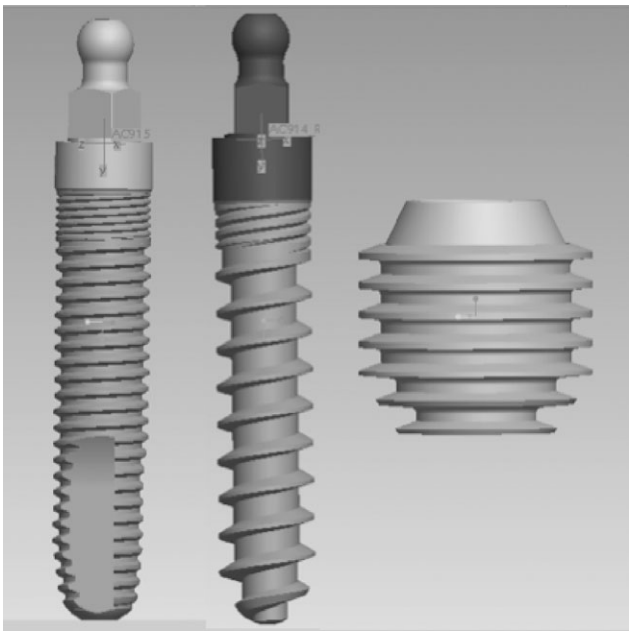

Figure 1 Short-pitch (*left*), large-pitch (*center*), and plateau (*right*) root shapes.

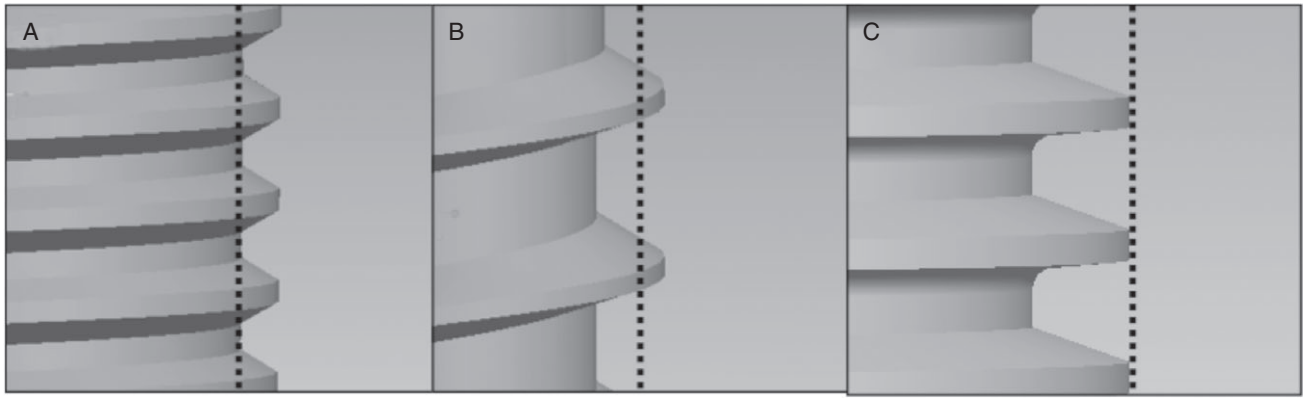

Figure 2 Implant macrostructure with respect to the final osteotomy diameter (*dashed lines*) for the (A) short-pitch implant (implant inner diameter equals the final osteotomy), (B) large pitch (implant inner diameter is 2.0 mm, and osteotomy is 2.5 mm in diameter), and (C) plateau.

medial–lateral position of the proximal tibiae. The remaining devices were placed along a distal direction at distances of 1 cm from each other along the central region of the bone. The left and right limbs provided implants that remained for 4 and 2 weeks in vivo, respectively. The animals, limbs, and surgical site distributions for the 2- and 4-week comparison for SP, LP, and P implant shapes resulted in an equal number ($n = 6$) of implants per group and implantation time.

All surgical procedures were performed under general anesthesia. The preanesthetic procedure comprised an intramuscular (IM) administration of atropine sulfate (0.044 mg/kg) and xylasin chlorate (8 mg/kg). General anesthesia was then obtained following an IM injection of ketamine chlorate (15 mg/kg).

Following hair removal by means of a sharp blade and antiseptic cleaning with iodine solution at the surgical and surrounding area, a 5-cm incision at the skin level was performed. Then, the periosteum was reflected and the proximal tibial plateau was exposed.

Three osteotomies were created along the bone at least 10 mm from each other from proximal to distal. For the SP and LP implants, the osteotomy was made by a 1.5-mm-diameter pilot drill followed by 2.0- and 2.5-mm-diameter burs at 1,200 rpm under saline irrigation. The implants were then driven into the osteotomy sites by means of a torque wrench until a torque of 20 Ncm was reached. For the P implant shape, the initial drilling was performed by a 2-mm-diameter pilot drill at 1,200 rpm under saline irrigation and slow speed sequential drilling with burs of 2.5-, 3.0-, 3.5-, 4.0-, and 4.5-mm diameter. The implants were then press fit into the osteotomies by manual pressure. A schematic representation of the relationship between the final osteotomy and implant dimensions is presented in Figure 2, where direct contact between the SP implant surface and the old bone occurred concurrent with implant placement, whereas healing chambers were created for the LP and P implant designs.

Standard layered suture techniques were utilized for wound closure (4-0 vicryl – internal layers, 4-0 nylon – the skin). Postsurgical medication included antibiotics (penicillin, 20.000 UI/kg) and analgesics (Ketoprophen, 1 mL/5 kg) for a period of 48 hours postoperatively. The euthanasia was performed by anesthesia overdose.

At necropsy, the upper third of the limbs were retrieved by sharp dissection, the soft tissue was removed by surgical blades, and the bones were fixed in 10% buffered formalin for 15 days. Each limb was then sectioned into three individual blocks with one implant in the center of each block.

The blocks were subsequently washed in running water for 24 hours and gradually dehydrated in a series of alcohol solutions ranging from 70 to 100% ethanol based on a previously described method.[15] Following dehydration, the samples were embedded in a methacrylate-based resin (Technovit® 9100; Heraeus Kulzer GmbH & Co., Wehrheim, Germany) according to the manufacturer's instructions. The blocks were then cut into slices (~300-μm thickness) aiming the center of the implant along its long axis with a precision diamond saw (Isomet 2000®; Buehler, Lake Bluff, IL, USA), glued to acrylic plates with an acrylate-based cement, and a 24-hour setting time was allowed prior to grinding and polishing. The sections were then reduced to a final thickness of ~30 μm by means of a series of SiC abrasive

papers (400, 600, 800, 1,200, and 2,400) in a grinding/polishing machine (Metaserv 3000®; Buehler) under water irrigation.

Transmitted light and polarized light microscopy (Leica DM4000™; Wetzlar, Germany) at various magnifications were used for bone histomorphology. The BIC was determined at ×50 to ×200 magnification by means of a computer software (Leica Application Suite™; Heerbrug, Switzerland). BIC statistical evaluation was performed by one-way analysis of variance at 95% level of significance along with Tukey's post hoc test for multiple comparisons.

RESULTS

Animal surgical procedures and follow-up demonstrated no complications regarding procedural conditions, postoperative infection, or other clinical concerns.

Qualitative evaluation of the biologic response showed intimate contact between cortical and trabecular bone for all implant designs at both implantation times, including regions that were in close proximity or substantially away from the osteotomy walls (see Figures 2 and 3). No significant differences in BIC ($p > .75$) were observed between the SP, LP, and P implant shapes at both 2 and 4 weeks implantation time (Table 1).

The toluidine blue-stained thin sections presented an appositional bone healing mode at regions where intimate contact existed between SP, LP, and P implant surfaces and bone immediately after placement (see Figure 3). These regions comprised the vast majority of the SP implant perimeter, the outer aspects of the LP thread, and the tip of the plateaus of the P implant shape. In contrast, the initial healing pattern observed for the LP and P implants' healing chamber, reflecting this combination of implant design and surgical drilling, followed an intramembranous-type healing mode with large amounts of newly formed woven bone (see Figures 3 and 4).

Temporal morphologic changes were observed for the different implant designs. At 2 weeks, the SP implants were primarily surrounded by woven bone throughout its perimeter (see Figure 3A), and initial signs of remodeling and lamellar bone formation were observed at 4 weeks implantation time (see Figure 3B). The same temporal change was observed for the regions of the LP and P implants that were in close proximity with the bone immediately after placement (regions where no healing chamber was formed).

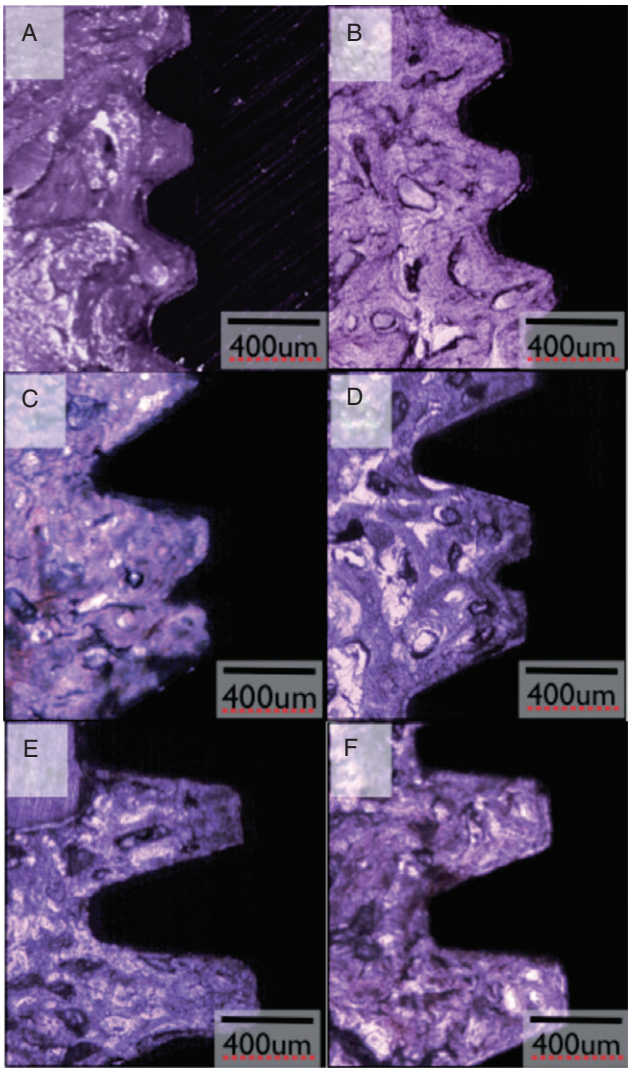

Figure 3 Toluidine blue-stained nondecalcified thin sections of short-pitch (SP) implants at (A) 2 weeks and (B) 4 weeks, large-pitch (LP) implants at (C) 2 weeks and (D) 4 weeks, and plateau (P) implants at (E) 2 weeks and (F) 4 weeks implantation time. At 2 weeks, newly formed woven bone was observed in direct contact with the surface of the different implant designs, and initial modeling sites were observed in the bone healing chambers of the LP and P implant designs. A qualitative increase in bone organization/maturation was observed for all implant designs at 4 weeks, where initial modeling/remodeling sites were observed in close proximity with the SP implant surface and throughout the chamber created due implant design + surgical drilling for the LP and P implants.

At 2 weeks, LP and P implant chambers were mostly filled with woven bone (see Figure 3, C and E), and initial modeling was also depicted with small amounts of lamellar bone surrounding a primary osteonic morphology. Further modeling was observed at 4 weeks, where the healing chambers of the LP and P implants showed multiple modeling sites and lamellar bone surrounding a rich vascular array (see Figure 3, D and F).[11]

TABLE 1 One-way Analysis of Variance Showing No Significant Differences ($p > .75$) in Bone-to-Implant Contact (BIC) for Short-Pitch (SP), Large-Pitch (LP), and Plateau (P) Implants at Both Implantation Times

Group	BIC (%)
2W SP	58.55 ± 12.2*
4W SP	72.27 ± 13.36*
2W LP	63.57 ± 12.2*
4W LP	54.45 ± 12.2*
2W P	58.84 ± 13.36*
4W P	66.91 ± 13.36*

W = weeks.
*Statistically homogenous group.

Polarized light microscopy at 2 weeks implantation time showed that a disorganized, nearly uniform in thickness (~150 µm) healing zone existed along the SP implant surface (see Figure 4A). Observations under polarized light mode revealed that a substantial amount of woven bone (shown darker on polarized mode because of its randomly organized morphology) was present at the healing chambers created between the LP implant threads or P implant plateaus (see Figure 4, B and C).

DISCUSSION

The bone healing process around screw root form implants is a well-known and established series of biologic events involving an initial inflammatory process around the implant surface, which is followed by deposition of new bone, modeling, and remodeling.[1,16] This process results in the anchorage of the implant device, which is prosthetically restored and presents treatment success rations often reported higher than 90%.[2,3,17,18]

On the other hand, different combinations of surgical drilling and implant designs (either plateau root form or screw root form) may result in void spaces between the implant and the osteotomy, which are filled with a blood clot immediately after implant placement.[11,19]

It has been previously demonstrated that after a few days, large blood clots filling large healing chambers[20] or the regions between bone and implant healing chamber walls[11,19] will evolve toward a provisional matrix of connective tissue presenting a high content of mesenchymal cells. The matrix adjacent to the drilled bone wall and along the implant surface will be substituted by woven bone trabeculae, and modeling/remodeling processes

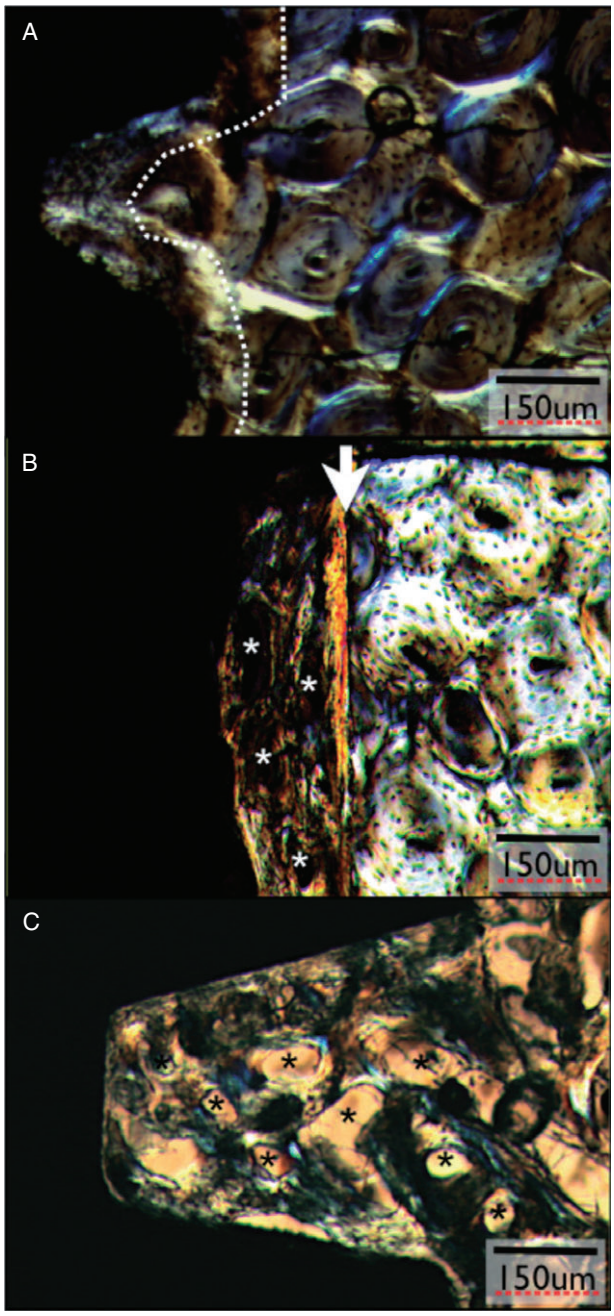

Figure 4 Polarized light microscopy of (A) short-pitch (SP), (B) large-pitch, and (C) plateau (P) implant designs at 2 weeks implantation time. The dashed line in A depicts the presence of newly formed woven bone along the perimeter of the SP implant to approximately 150 µm from the implant surface until reaching the osteonic region of the old cortical bone. The sharp line depicted along the arrow direction in B corresponds to the transition between the healing chamber and the osteonic region of the old cortical bone. Note the presence of blood vessels/trabecular spaces (*) within the healing chamber region. The bone structure presented in C corresponds to the healing chamber of the P implant, where blood vessels/trabecular spaces (*) are surrounded by bone presenting higher polarized light transmittance as a result of microstructural alignment, suggesting the onset of initial modeling of the woven bone microstructure presented throughout the chamber as dark regions because of its lack of organization.

will result in more mature fiber-aligned lamellar bone.[11,19] Such pattern of healing may cause a callus-like healing phenomenon, possibly responsible to a rapid biomechanical stabilization of the implant.[14]

The histomorphometric results showed that regardless of the implant and surgical drilling utilized, high degrees of BIC were observed at both 2 and 4 weeks in vivo, supporting that the implant surfaces utilized in the present study were biocompatible and osteoconductive.[6,7,21] Specific to the healing chamber models, where surface chemistry[7,19] and hydrophilicity[7] have been shown to play a significant role on inicial healing versus different control surfaces, no significant differences in %BIC were observed between the LP (dual acid-etched surface) and the P (alumina-blasted/acid-etched) implants at both evaluation times. Thus, despite previously reported differences in surface roughness between dual acid-etched and grit-blasted and acid-etched surfaces (typically rougher than dual acid-etched surfaces[4,6]), the experimental model and time frames used in the present study were not able to determine BIC differences between the healing chambers' implant surfaces. It should also be noted that BIC is an indicator of implant surface biocompatibility and osteoconductivity, and the final implant in bone biomechanical fixation is a function of the combination of BIC, the mechanical properties of the bone surrounding the implant, implant design, and load nature.[14]

Despite the characteristic differences in healing pathway among the groups, where larger amounts of woven bone were required to fill the LP and P implants healing chambers, similar bone morphology evolution was depicted for all implant groups. Thus, the initial signs of woven bone resorption/modeling observed at 2 weeks and its further evolution at 4 weeks suggest that healing kinetics was similar and that bone maturation and mechanical properties achievement may occur in the same temporal frames.[19] However, because of the different implant configurations and amounts of woven bone at different time frames, varied degrees of biomechanical stability may occur and further investigation concerning bone mechanical properties assessment are desirable to determine potential benefits of one implant design and surgical drilling over the other.

CONCLUSIONS

Based on the results obtained, it was possible to conclude that all materials used in this experiment fulfill their claims of biocompatibility and osteoconduction. Also, although different implant designs and associated surgical techniques leading to varied degrees of initial stability, interaction between bone and biomaterial, no significant differences were observed in bone-to-implant between groups. Finally, regardless of the combination between implant design and final osteotomy drilling, bone morphology evolution from 2 to 4 weeks was comparable.

REFERENCES

1. Albrektsson T, Branemark PI, Hansson HA, Lindstrom J. Osseointegrated titanium implants. Requirements for ensuring a long-lasting, direct bone-to-implant anchorage in man. Acta Orthop Scand 1981; 52:155–170.
2. Chuang SK, Tian L, Wei LJ, Dodson TB. Kaplan-Meier analysis of dental implant survival: a strategy for estimating survival with clustered observations. J Dent Res 2001; 80:2016–2020.
3. Chuang SK, Wei LJ, Douglass CW, Dodson TB. Risk factors for dental implant failure: a strategy for the analysis of clustered failure-time observations. J Dent Res 2002; 81:572–577.
4. Albrektsson T, Wennerberg A. Oral implant surfaces: part 2 – review focusing on clinical knowledge of different surfaces. Int J Prosthodont 2004; 17:544–564.
5. Branemark PI. Osseointegration and its experimental background. J Prosthet Dent 1983; 50:399–410.
6. Albrektsson T, Wennerberg A. Oral implant surfaces: part 1 – review focusing on topographic and chemical properties of different surfaces and in vivo responses to them. Int J Prosthodont 2004; 17:536–543.
7. Buser D, Broggini N, Wieland M, et al. Enhanced bone apposition to a chemically modified SLA titanium surface. J Dent Res 2004; 83:529–533.
8. Butz F, Aita H, Wang CJ, Ogawa T. Harder and stiffer bone osseointegrated to roughened titanium. J Dent Res 2006; 85:560–565.
9. Coelho PG, Cardaropoli G, Suzuki M, Lemons JE. Early healing of nanothickness bioceramic coatings on dental implants. An experimental study in dogs. J Biomed Mater Res B Appl Biomater 2009; 88(2):387–393.
10. Yang Y, Kim KH, Ong JL. A review on calcium phosphate coatings produced using a sputtering process – an alternative to plasma spraying. Biomaterials 2005; 26:327–337.
11. Berglundh T, Abrahamsson I, Lang NP, Lindhe J. De novo alveolar bone formation adjacent to endosseous implants. Clin Oral Implants Res 2003; 14:251–262.
12. Davies JE. Understanding peri-implant endosseous healing. J Dent Educ 2003; 67:932–949.
13. Davies JE. Mechanisms of endosseous integration. Int J Prosthodont 1998; 11:391–401.

14. Lemons JE. Biomaterials, biomechanics, tissue healing, and immediate-function dental implants. J Oral Implantol 2004; 30:318–324.
15. Donath K, Breuner G. A method for the study of undecalcified bones and teeth with attached soft tissues. The Sage-Schliff (sawing and grinding) technique. J Oral Pathol 1982; 11:318–326.
16. Roberts WE. Bone tissue interface. J Dent Educ 1988; 52:804–809.
17. Chuang SK, Hatch JP, Rugh J, Dodson TB. Multi-center randomized clinical trials in oral and maxillofacial surgery: modeling of fixed and random effects. Int J Oral Maxillofac Surg 2005; 34:341–344.
18. Chuang SK, Tian L, Wei LJ, Dodson TB. Predicting dental implant survival by use of the marginal approach of the semi-parametric survival methods for clustered observations. J Dent Res 2002; 81:851–855.
19. Berglundh T, Abrahamsson I, Albouy JP, Lindhe J. Bone healing at implants with a fluoride-modified surface: an experimental study in dogs. Clin Oral Implants Res 2007; 18:147–152.
20. Cardaropoli G, Wennstrom JL, Lekholm U. Peri-implant bone alterations in relation to inter-unit distances. A 3-year retrospective study. Clin Oral Implants Res 2003; 14:430–436.
21. Branemark PI, Adell R, Breine U, Hansson BO, Lindstrom J, Ohlsson A. Intra-osseous anchorage of dental prostheses. I. Experimental studies. Scand J Plast Reconstr Surg 1969; 3:81–100.